CI&CEQ
Chemical Industry & Chemical Engineering Quarterly

Available online at
Association of the Chemical Engineers of Serbia AChE
www.ache.org.rs/CICEQ

*Chem. Ind. Chem. Eng. Q.* 31 (3) 173–184 (2025) CI&CEQ

KARTHIKEYAN SUBRAMANIAN[1]
SATHIYAGNANAM AMUDHAVALLI PARAMASIVAM[2]
DAMODHARAN DILLIKANNAN[3]

[1]Department of Mechanical Engineering, Annamalai University, Chidambaram, Tamil Nadu, India

[2]Department of Mechanical Engineering, Govt. College of Engineering (Deputed from Annamalai University), Salem, Tamil Nadu, India

[3]Department of Mechanical Engineering, Jeppiaar Engineering College, Chennai, Tamil Nadu, India

SCIENTIFIC PAPER

UDC 662.756.3:621.4:519.7

# MACHINE LEARNING PREDICTIONS ON THE OUTPUT PARAMETERS OF COMMON RAIL DIRECT INJECTION ENGINES FUELED WITH TERNARY BLEND

## Article Highlights

- CRDI engine performance with a methyl acetate antioxidant/Non-edible oil/diesel ternary blend
- Examine the impacts of fuel injection strategies (FIT and EGR) on the engine characteristics
- Innovation of machine learning algorithms and prediction models LR, NN, K-NN, SVM, and LSTM.
- The LSTM model yields the highest $R^2$ value range of 0.92 to 0.96, for each engine response

## Abstract

*This study aims to employ a machine learning algorithm (MLA) to predict Common Rail Direct Injection (CRDI) engine emissions and performance using alternative feedstock. This study started with a diesel-SCOME- Methyl Acetate ternary mix. The engine was tested with fuel injection time (FIT) of 23°, 21°, and 19° bTDC with exhaust gas recirculation (EGR) levels of 10%, 15%, and 20% at estimated power productivity. Retard injection time and increasing EGR rates reduced in-cylinder peak pressure. Operating conditions with the maximum BTE were 21° bTDC and 10% EGR. Adjusting injection time and EGR reduced nitrogen oxide relative to the baseline. Smoke opacity was 1% lower at 21° bTDC and 10% exhaust gas recirculation than in conventional diesel operation. Retard injection time and exhaust gas recirculation increased HC and CO emissions. However, MLAs predict CI engine operation and discharge properties. The long short-term memory (LSTM) Model predicts engine output characteristics with a squared correlation ($R^2$) of 0.92 to 0.96. At the same time, mean relative error (MRE) values ranged from 1.74 to 4.68%. These results show that the LSTM models provide superior predictive capabilities in this investigation, particularly when considering numerous variables to analyze engine responses.*

*Keywords: biodiesel; methyl acetate; CRDI engine; EGR; Machine Learning Algorithms.*

Fossil fuel-based energy use in industrialized and developing nations is predicted to grow by 5–7% and 1–2% yearly. In response to this increasing use, researchers are considering alternative resources [1]. Because of their contributions to significant sectors, diesel engines are vital to the world market consequently [2]. Because they are more effective at transforming fuel than gasoline engines, compression ignition (CI) engines are often used in mobility. Nevertheless, because of their harmful impacts that affect the ecology and individual wellness, the greater levels of pollutants are a cause for worry. Prolonged exposure to pollutants has been found to elevate the likelihood of developing lung cancer, increasing the susceptibility to cardiorespiratory ailments [3]. It is feasible to use several types of oils to power CI engines

Correspondence: K. Subramanian, Department of Mechanical Engineering, Annamalai University, Chidambaram, Tamil Nadu, India.
E-mail: karthikeyanphd2022@gmail.com
Paper received: 30 March, 2024
Paper revised: 24 June, 2024
Paper accepted: 2 July, 2024

https://doi.org/10.2298/CICEQ240303025S

by using numerous methods and making adjustments [4]. The study reported that biomass fuel for industrial use is derived from agricultural byproducts. Thus, environmental impacts are mitigated. The effects of varying the ratio of alcohols added to milk scum oil are analyzed [5].

### Overview of *Simmondsia chinensis* feedstocks

It is reported that the *Simmondsia chinensis* oil (SCO) extract from the seeds of the Jojoba tree plant, a shrub can reach a height of between 1 and 5 m and has a long, healthy life span (100–200 years). This plant, which is common in the United States, has many other names. Its seedlings have oil and wax content ranging from 44 to 56 percent. The jojoba oil had a yellow hue, was without scent, and contained only trace amounts of triglyceride esters in addition to 97% monoesters of long-chain lipids. This chemical component is responsible for jojoba's self-stability and tolerance to elevated temperatures when compared to other non-edible oils [6]. When SCO is treated with the transesterification procedure, the result is biodiesel, which has improved properties than plain diesel, such as greater intrinsic oxygen content, improved cetane, and less sulfur [7].

### Biodiesel as an alternative fuel in CI Engine

Researchers evaluated CI engine efficiency and conducted ignition experiments using biodiesel derived from palm oil. It was discovered that using warmed oil resulted in decreased hydrocarbon (HC) and carbon monoxide (CO) pollutants but greater exhaust temperatures and nitrogen oxide (NOx) levels. Hydrous ethanol significantly reduces nitrogen oxide emissions, according to a critical analysis of numerous approaches to employing it in engines [8]. Results from the experiments demonstrated a drastic cut in various discharges compared to the diesel engine running on a single injection. In addition, growth in brake thermal efficiency (BTE) was 4.46%. Propane-inducing diesel engines using waste seed biodiesel (WSBD) have been investigated [9]. Additionally, this revolutionary combustion method is being heavily tested in internal combustion engines. Minimizing pollutants and increasing burning effectiveness are the objectives [10]. Another study examined the effects of using sapota methyl ester on the parameters of combustion and EGR and their impact. The outcomes suggested that shorter delays occurred at higher CR values. Lowered levels of nitrogen oxides were also detected [11]. The trial was conducted using cottonseed biodiesel in a common rail direct injection (CRDI) engine using exhaust gas recirculation. It follows from these experimental probes that an EGR rate of 25% results in a nearly 33% reduction in Nox [12]. Recently, the binary combination concept was investigated as a result of superior blend stability, reduced expenditure, along minor changes in engine hardware settings. The research outlined in this paper attempts to use gasoline along with methyl acetate. The studies on methyl acetate additives in engine applications are very limited. They have achieved prominence because of their soot minimization capability [13].This study looks at what happens when diesel and n-Pentanol/Karanja oil biodiesel are mixed. By including n-Pentanol, the properties of the biodiesel-diesel blend will be better at low temperatures. Pentanol's reduced fluidity and great instability will also significantly lower pollutants [14]. They discovered that a higher concentration of additives significantly decreased brake-specific fuel consumption (BSFC) and contributed to a steeper percentage decline in emissions [15].

### Studies on variable FIT and EGRs with Ternary fuel

The experiment was carried out with a ternary combination of diesel and JME+ n-butanol additive. It can be shown that jojoba oil with a high fraction of DBJ15 has the potential to achieve reduced pollutants in the short term while maintaining a high thermal efficiency [16]. Alcohol is made from a vast range of environmentally friendly ingredients. Alcohols, which include methanol, ethanol, and propanol, have a lower number of carbon atoms. Higher alcohols, on the other hand, have more carbon atoms than lower alcohols. These include pentanol, hexanol, heptanol, and decanol [17]. Researchers investigated the effects of combining diesel with 1-hexanol at different injection times and EGR percentages. Integrating 1-hexanol with an improved pre-combined burning phase prolonged the ignition impediment's length. At 23 BTDC and 10% EGR, there was a systematic reduction in both NOx and smoke [18]. The usage of EGR technology is one common strategy for decreasing exhaust-borne nitrogen oxides in IC engines [19]. Increase the ratio of 1-$C_6H_{14}O$ in diesel/WPO blends. Based on the data, it was found that an increased 1-$C_6H_{14}O$ fraction in the mixture somewhat reduced engine performance. Smoke, CO, and NOx were reduced at the same duration, although there was a small increase in hydrocarbons [20]. Investigators conducted an empirical analysis of 2 greater alcohols, decanol and 1-hexanol, combined with various blends of diesel and biodiesel. In this case, the tertiary mixes were almost identical to pure diesel and had superior BTE than biodiesel. Because of the greater alcohol content, the tertiary mix has the minimum emission characteristics, such as the least amount of smoke emission [21]. It stipulates that a CRDI diesel engine running on a ternary mix fuel has its burning and exhaust properties carefully examined during reduced passive

configurations. As a result, there is a decrease in smoke and Nox discharges. In addition to being very unpredictable, ethanol has an elevated level of $O_2$ and an elevated latent heat of evaporation. Any of these actions might aid in lowering smoke and NOx pollutants [22]. Because ABE-diesel blends have a bigger $O_2$ level and latent heat of vaporization than plain diesel, the ABE-diesel operating attributes in a CO engine considerably reduce the production of soot particles and increase ultimate particle degradation. Additionally, a greater amount of air may be drawn into the spray from upstream due to the prolonged flame lift-off duration and ignition latency period [23].

### Overview of machine learning prediction

In recent years, the field of machine learning has made a lot of progress, and techniques like artificial neural networks (ANN), support vector machine (SVM), random forest (RF), extreme gradient (XG) Boost, and deep neural networks (DNN) have emerged rapidly [24]. Integrating engine research with machine learning modeling methodologies can enhance the calibration of the engine and the identification of the effective zone and minimize the trials and 3D simulations [25]. Machine learning (ML) is one of the cutting-edge developments in the field of artificial intelligence (AI). Machine learning algorithms (MLAs) are plentiful; they all involve the same repetitive application of mathematical formulas [26]. MLAs are classified into four distinct categories, which are very significant [27]. In MLAs, the unsupervised learning technique is used to identify the hidden pattern of data when a training dataset is not available for investigation. The supervised learning method is used to anticipate data patterns when a designated training dataset is available. When some pieces of information are missing from the training dataset, supervised learning can be transformed into semi-supervised learning. When analyzing a data pattern and receiving input from an outside source, MLAs use the reinforcement learning technique [28]. The use of AI in bioenergy processes is extremely limited. In addition, there is a shortage of research that addresses the potential of machine learning techniques for making predictions and enhancing efficiency. Researchers have found that ML shows considerable promise for overcoming obstacles to expanding bioenergy production [29]. There is also a lack of data on the effectiveness of methyl acetate and biodiesel in CI engines. Therefore, this article uses ternary fuel to address these gaps in the literature. The ternary fuel has been compared on several important metrics. These performance parameters are predicted using cutting-edge ML methods.

### Significance of the present work

Contrary to the existing literature, this study ventures into unexplored territory by examining the potential of methyl acetate additives as a viable substitute in CI engines. It goes beyond the limited studies on the impact of methyl acetate inclusion in diesel and *Simmondsia Chinensis* oil methyl ester (SCOME) combinations and explores the influence of EGR and injection time with variable projection using various ML systems. The objective is to employ these algorithms in analyzing the emission and performance attributes of a diesel engine operating on blends of methyl acetate-diesel fuel fortified with antioxidants. This research conducts a comprehensive analysis to evaluate the predictive performance of neural networks, k-NN, support vector machines, linear regression (LR), and Long Short-Term Memory (LSTM) methods in comparison to commonly employed techniques. The evaluation is based on the $R^2$ metrics. This paper proposes the utilization of a deep learning algorithm, namely an LSTM model, as a novel approach for predicting engine emissions and performance.

## MATERIAL AND METHODS

### Evaluation of test samples

Table 1 lists the key features of biofuel derived from *Simmondsiaceae* shrub seedlings, as well as the assessment variants. Because of the elevated fluidity and content of the SCO, its simple usage may result in injection problems. As a result, the transesterification process was modified in the conversion of SCO to reduce its consistency and concentration. Merck Millipore supplied $C_3H_6O_2$. A ternary mixture of $C_3H_6O_2$, diesel, and biodiesel was created. By combining diesel with biodiesel, binary variation was created. The diesel content in the two combinations was 70% and 50%, accordingly. The ternary blends were referred to as D50SCOME30MA20 (Diesel 50% + SCOME30% + Methyl Acetate 20% by volume) is the MA20 blend. D70SCOME30 (Diesel 70% + Biodiesel 30% by volume) is the binary combination.

### Experimentation equipment and configuration

Figure 2 depicts the experimental configuration. The Kirloskar TV1 CI engine was used for evaluation, which was a mono-cylinder, 4S, VCR-CI engine coupled to a dynamometer. In compliance with Nira i7r rules, it was restructured with the requisite receptors, sensors, and an accessible ECU to provide electronic injection. An AVL DIGAS 444N tester was used for determining NOx, while an AVL 437C smoke meter was used to detect smoke (SO). To achieve the injection

*Table 1. Characteristics of test fuels.*

| Property | Standard | Diesel | SCOME | D70 SCOME30 | D50 SCOME30 MA20 |
|---|---|---|---|---|---|
| Density (kg/m$^3$) | ASTM | 832 | 877 | 846 | 873 |
| Kinematic viscosity @40°C (cst) | ASTM D 445 | 2.89 | 5.12 | 3.85 | 3.51 |
| Flash Point (°C) | ASTM D 92 | 69 | 152 | 96.9 | 98.7 |
| Cetane Index (CI) | ASTM D 976 | 47 | 51 | - | - |
| Calorific Value (MJ/kg) | ASTM D 240 | 42.5 | 38.21 | 41.28 | 39.12 |

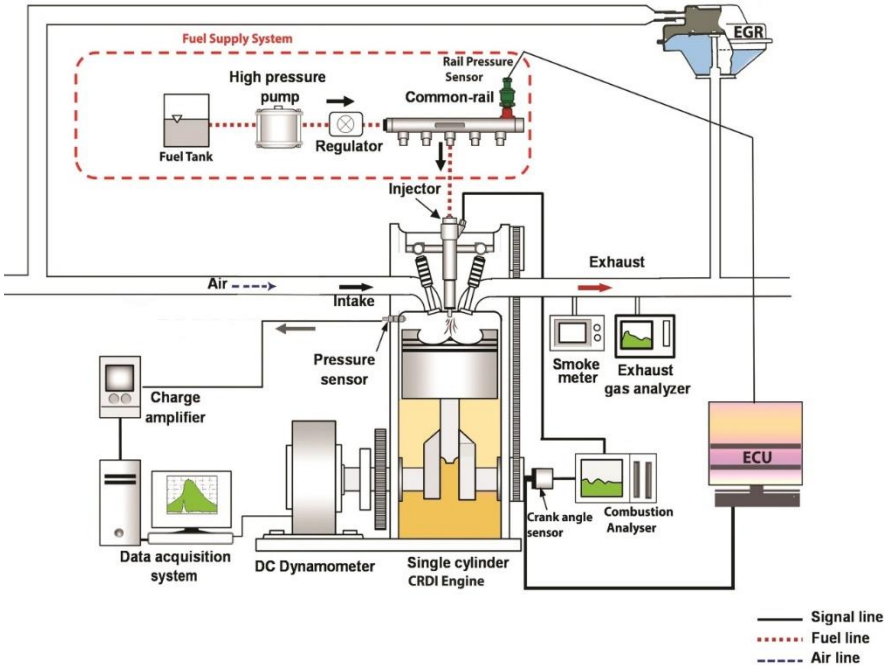


*Figure 1. Schematic layout of experimental setup.*

parameters needed for the assessment, a CRDI was required. The diesel delivery line was changed to link to the CRDI framework, and a high-pressure pumping was added to the fuel filtration. This serves as both a diesel holding reservoir and a pressure controller for the injection equipment. To regulate pressure, a rail pressure sensor is connected to the Nira i7r ECU. Although the original injector was unable to manage the much-increased injection pressures used by CRDI, a 6-hole solenoid-regulated nozzle was chosen to complete the job. The ECU was used to alter the first sensors and actuators to guarantee that every part worked properly. If the engine runs properly, it is termed diagnostically competent. Table 2 summarises the experiment engine settings.

*Table 2. Technical specification.*

| Make and Model | Kirloskar, TV1 |
|---|---|
| Cylinders & Stroke | 1 & 4 |
| Bore | 87.5 mm |
| Stroke length | 110 mm |
| Swept volume | 661 cc |
| Speed | 1500 rpm |
| Rated output | 3.5 kW at 1500 rpm |
| CR | 1:17.5 |
| Cooling method | Water-cooled |
| IT, CA bTDC | 23° |
| FIP | 600 bar |

## EGR Setup

The EGR method is used to lower the in-cylinder and total temperatures of the charge, which in turn diminishes the emissions of $NO_X$. This also makes EGR denser, which means its overall volume increases. A portion of the outlet gas is routed via the exhaust gas recirculation cooler and then into the air inlet. As the $H_2O$ in the exhaust gas recirculation cooler stays at the same temperature, it functions as a thermal replacer, taking in the heat from the outlet gases that are being held back. Here, the discharge was subjected to a temperature reduction of 36 °C. The EGR valve regulates the amount of air that is recycled through the engine. The orifice size determines the exhaust gas flow rate. The best way to start the operation was to send the recycled exhaust gas to the input port. Eq. (1) was used to calculate the amount of EGR rate.

$$EGR\% = \left[\frac{(CO_2)_{\text{int}ake}}{(CO_2)_{exhaust}}\right] \times 100 \quad (1)$$

The AVL 444 N gas equipment, renowned for its precision, was implemented to determine the amount of $CO_2$ being released. This was achieved by adjusting the outlet discharge until the amount of incoming

carbon dioxide met a certain value, ensuring accurate measurements. [30].

### Experimental procedure

The baseline emissions and performance characteristics from the perspective of replacing 50% of the diesel volume with biodiesel. Tests were conducted on a binary blend that contained 70% diesel and 30% biodiesel. Compared to baseline diesel, smoke emissions were greater, and performance was worse. Therefore, we employed a well-established additive-blending approach to reduce tailpipe smoke below diesel operation levels. The methyl acetate was chosen for this study because of its similar properties to diesel. The study aims to replace 50% of the volume of diesel with an alternative fuel. We kept the diesel volume constant, lowered the biodiesel by 20% vol., and balanced it with methyl acetate. The ternary mix included 50% diesel, 30% SCOME, and 20% methyl acetate. Compared to the binary option, the ternary mix operation improved combustion and reduced smoke emissions below diesel. But the ternary blend did more tests at full load, changing the fuel injection time (FIT) (23°bTDC, 21°bTDC, and 19°bTDC) and the exhaust gas recirculation (10%, 15%, and 20%) to find the best setting for lowering NOx and smoke emissions, as well as producing better performance. The study used diesel, two binary, and one ternary blend at normal operating conditions of 23º bTDC without EGR. Based on the examination, the ternary blend (D50SCOME30MA20) gave the best performance among the other blends at a normal setting. It is nearly closer to baseline fuel. Consequently, we conducted enhancement tests on the ternary blend of D50SCOME30MA20 (MA20) at compression ratio (CR19), and injection pressure (IP 600 bar) remained constant. Conducted the three trials on the same day and in the same weather conditions to establish consistency.

### Machine Learning (ML) algorithms

ML is a recurrently employed form of AI technique. Artificial intelligence (AI) is widely regarded as an appealing and widely embraced technology for its ability to effectively identify and address various application domains, owing to its exceptional capacity for achieving high levels of accuracy [27]. The system is designed to possess the capacity for autonomous observation and subsequent prediction of unknown reactions. Without a doubt, user attributes and the success of their training have a direct impact on the effectiveness of ML algorithms [29]. The current study delves into a comprehensive analysis of 4 distinct ML algorithms. The four machine learning models discussed in this context are LR, neural networks (NN), SVM, and LSTM. All algorithms are executed with Rapidminer Studio Version 9.6. The grid investigation methodology is employed in this research to predict the model parameters. The algorithms employed in this study are utilized to forecast engine responses, namely BSEC and BTE, as well as NOx, CO, HC, and smoke. During the training process, three specific inputs are utilized, namely engine test fuels, FIT, and EGR rates. The study utilized a dataset including nearly 288 data points. The dataset was partitioned randomly using the shuffled sample technique in the methods. The training phase of the algorithms utilized 80% of the available data points, while the remaining 20% was allocated for the testing phase.

## ANALYSIS OF ENGINE OUTPUT PARAMETERS

### Combustion investigation

#### *In-cylinder pressure analysis*

Figure 2 illustrates the in-cylinder pressure (ICP) discrepancies observed at various crank angle (CA) sites for the examined variations. Under the same circumstances, Diesel, D70SCOME30, D50SCOME50, and D50SCOME30MA20 were 69.96, 69.82, 69.29, and 69.80 bars. The extended ignition delay of the MA20 variation, where more fuel ignites impulsively, led to a higher ICP compared to the binary combination. At 23°, the PCPs for 10%, 15%, and 20% exhaust gas recirculation were 69.29, 68.99, and 67.55 bar. At FITs of 21° and 19°, the ICPs for exhaust gas recirculation levels of 10%, 15%, and 20% were 66.04 bar, 66.95 bar, 65.19 bar, 62.99 bar, 61.69 bar, and 60.46 bar. Retarding FIT from 23° to 19° at any exhaust gas recirculation rate results in a drop in the ICP. At 10% EGR, the ICP decreased by 9%. Delayed ignition reduces fuel burning due to the bTDC drop, resulting in less uniform volume ignition and a lower ICP [31]. The EGR levels are enhanced from 10% to 20%, and PCP is reduced further at any given injection timing. For instance, at FIT of 23°bTDC, the PCP dropped by 2.5%. This is because the discharge emissions increased the specific heat, leading to a decrease in PCP [17].

### Heat release rate analysis (HRR)

Figure 2b reveals HRR disparities at different crank inclinations for the evaluation fuels. The HRR for Diesel, D70SCOME30, D50SCOME50, and D50SCOME30MA20 were 45.63 J/°, 43.08 J/°, 40.43 J/°, and 48.13 J/°, correspondingly. Here, the MA20 blend portrayed higher HRR, which is resultant of the collective effect of lengthier ignition duration and better-oxygenated circumstances that increase the flame speed in the course of combustion, resulting in elevated HRR values [32]. When Increasing EGR

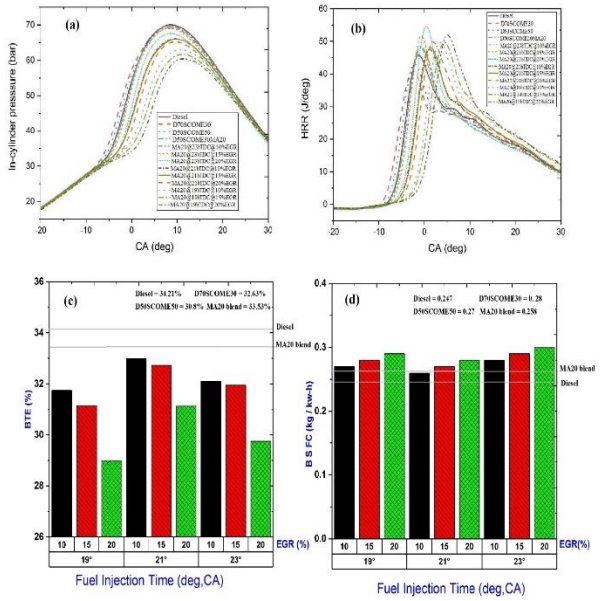


*Figure 2. (a) ICP, (b) HRR, (c) BTE, and (d) BSFC for MA20 variant at various FIT and EGR rates.*

levels and decreasing injection time cause the HRR graph to shift from left to right. EGR levels of 10%, 15%, and 20% at 23° have heat release rates of 48.51 J/°, 51.21 J/°, and 53.84 J/°. Similarly, for FIT values of 21° and 19°, HRRs are 47.56 J/°, 47.73 J/°, 49.93 J/°, 49.42 J/°, 49.45 J/°, and 52.07 J/° at EGR rates of 10%, 15%, and 20%. When changing the injection time from 23° to 21°, the HRR's peak point decreased. The HRR decreased from 48.51 to 47.56 J/° at 10% EGR. The decrease in injection time from 21° to 19° increased HRR. Due to a decrease in injection time, the FIT retards from 23° to 21°, reducing premixed combustion fuel usage. This reduces fuel consumption and increases heat release.[33]. A longer ignition delay due to retarded FIT increased the early mixed-period burning percentage and HRR excesses. HRR optimization occurred when EGR rose from 10% to 20%. HRR improves by 10% at 23°, but EGR rises from 0% to 20%. The EGR's impact prolongs ignition lag. The increase is due to the preliminary mixed-burning step using supplemental fuel. Similar findings were reported. [20].

## Performance investigation

### *Brake thermal efficiency*

Figure 2c shows the D50SCOME30MA20 blend's brake thermal efficiency at various FIT and exhaust gas recirculation settings. Diesel, D70SCOME30, D50SCOME50, and D50SCOME30MA20 had BTEs of 34.21%, 32.63%, 30.80%, and 33.53% at optimal output and engine standard specifications. The D50SCOME30MA20 mix had 2.3% greater BTE than the D50SCOME50 blend due to improved low heating value, atomization, and inborn $O_2$, which accelerated combustion. Biodiesel ignites faster, especially during flame expansion, due to its higher thermal potential and oxygen content. [34]. The value of BTE is 32.12%, 31.96%, and 29.75% at 23° with EGR settings of 10%, 15%, and 20%. The BTE is 33%, 32.73%, 31.14%, 31.75%, 31.16%, and 28.99% at 21° and 19° FITs. According to Figure 2c, the tertiary mix delivered at 21° had the highest BTE, 2.5% more than that provided at 23° at the same EGR level. HRR studies support this. The ternary mix at 21° bTDC recovers more outputs and dissipates thermally faster, increasing BTE. Extended exhaust gas recirculation lowers the thermal efficiency of the ternary mix brake system. Because exhaust gases hinder combustion, BTE is lower [30].

## Brake-specific fuel consumption

Brake-specific fuel consumption (BSFC) is a crucial measure of fuel efficiency for engines that generate rotational power. It quantifies how effectively the engine converts fuel into work, making it a key metric in our study. The BSFC measure's calorific value (CV), a significant biodiesel property, plays a vital role in this process. Reduced calorific values increase fuel consumption to provide the same power output; therefore, higher CVs reduce BSFC, indicating better fuel efficiency [35]. It's important to note that although BTE and BSFC have an adverse connection, diesel with a reduced BTE has a higher BSFC. As a consequence, the rationale for the changes in BTE among biodiesel, biodiesel-alcohol combinations, and diesel applies to BSFC as well. This reaffirms the scientific rigor and validity of our research. [21]. Figure 2d provides a practical perspective, showcasing the D50SCOME30MA20 variant's BSFC at different FIT and exhaust gas recirculation levels. Diesel, D70SCOME30, D50SCOME50 combination, and D50SCOME30MA20 mixture had BSFCs of 0.247, 0.28, 0.27, and 0.258 kg/kW-hr at stated capacity and engine standard characteristics. D50SCOME30MA20 has a lower BSFC than D50SCOME50. Due to its higher $O_2$ and CV, the ternary type uses less fuel to create similar energy. At 23° bTDC, the engine's BSFC was 0.28, 0.29, and 0.31 kg/kW-hr for 10%, 15%, and 20% EGR. At 10%, 15%, and 20% EGR, the engine's BSFC was 0.264, 0.272, 0.282, 0.273, 0.28, and 0.291 kg/kW-hr at FITs of 21° and 19°. Initially, the tertiary mixture BSFC dropped. We found that delaying the FIT from 23° to 21° and then to 19° increased it. Since the FIT was adjusted from 23° to 21°, this happened. This improvement allowed full burning by locating the combustion process at TDC. Thus, the engine needed less power to reach the speed. Lowering FIT from 21° to 19° caused heat dissipation lowered output and increased BSFC during the expansion stroke. For the ternary mix, higher EGR was

due to deterioration, which changed the air-fuel proportion and reduced burning, increasing BSFC. [19].

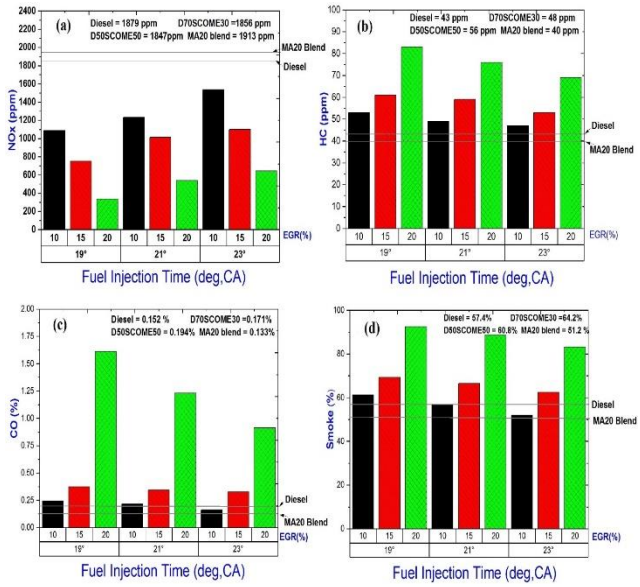


*Figure 3. (a) NOx, (b) HC (c) CO, and (d) Smoke for MA20 at different FIT and EGR levels.*

## Exhaust analysis

### *NOx emission*

Figure 3a shows nitrogen oxide differences for the D50SCOME30MA20 mix at different FIT and EGR levels. Diesel, D70SCOME30, D50SCOME50 mix, and D50SCOME30MA20 blend emitted 1859, 1856, 1847, and 1913 ppm of NOx under specified power circumstances and engine stock settings. The ternary mix emitted more NOx than the binary form because methyl acetate stimulates burning, raising gas temperatures and NOx. Biodiesel burns more thoroughly due to its high oxygen content, raising peak temperatures and NOx emissions [36]. Concerning EGR values of 10%, 15%, and 20%, at 23° bTDC, the NOx emission was 1536, 1100, and 642 ppm, correspondingly. Similarly, at a FIT of 21° bTDC and 19° bTDC, the nitrogen oxide values were 1231 ppm, 1012 ppm, 540 ppm, 1088 ppm, 753 ppm, and 335 ppm, respectively, at EGR rates of 10%, 15%, and 20%. Delaying injection until 19° bTDC instead of 23° bTDC significantly reduced NOx emissions. The exhaust gas recirculation rate was set at 10%, and the injection time was reduced from 23° to 21° bTDC, reducing NOx emissions by 17%. Delaying the FIT reduced NOx by 30%. The original analysis found that a ternary mix at 21° bTDC increased centralized burning. A shorter ID time and lower fuel consumption helped keep nitrogen oxides low [35]. The retardation of the explosive process by 21° to 19° bTDC displaced the combustion mechanism, changing the TDC point. This improvement allowed LTC mode adoption, reducing nitrogen oxide emissions significantly [22]. The charge mixture's oxygen concentration disproportionately affected NOx formation, which accelerated chemical processes and boosted combustible temperatures. The charge mixture's oxygen content affected NOx production. Raising the EGR rate from 10% to 20% for a certain injection period reduced NOx output by more than twice. The dilutive impact of increased thermally sensitive exhaust gases reduced exhaust temperatures [37]. In addition, the chemical reaction speed was impacted by the restricted supply of $O_2$.

### *Hydrocarbon*

Figure 3b shows the D50SCOME30MA20 variant's HC at different FITs and EGRs. HC emissions at specified power output and engine settings for Diesel, D70SCOME30, D50SCOME50 mix, and D50SCOME30MA20 blend had HC emissions of 42, 48, 56, and 40 ppm, respectively. This shows that ternary variants reduce HC. In the diesel/SCOME combination, methyl acetate increased $O_2$ levels. This sped up the oxidation reaction even in areas with a lot of fuel, breaking down HCs that were not fully depleted and lowering HC emissions. At 23° bTDC, HC emission was 47, 53, and 69 ppm for 10%, 15%, and 20% EGR. In the same way, HC emission was 49 ppm at FITs of 21° bTDC and 19° bTDC, 59 ppm at 76° bTDC, and 53, 61, and 83 ppm at 10%, 15%, and 20% EGR rates. Increasing exhaust gas recirculation (EGR) to 10% and fuel injection time (FIT) from 23° to 19° bTDC increases hydrocarbon (HC) emissions by 11%. Because of the delayed injection, the membrane was more likely to get wet, and fuel was held in poor combustion zones. This produced unburned or partially burned HC [30]. Increasing EGR intensity from 10% to 20% resulted in increased HC emissions. This tendency to release HC is caused by exhaust gases lowering the gas temperature. This makes it difficult for hydrocarbons to split into carbon particles, releasing more HC [31].

### *Carbon monoxide*

Figure 3c shows CO emission differences in the D50SCOME30MA20 blend at different FIT and EGR settings. Diesel, D70SCOME30, D50SCOME50 mix, and D50SCOME30MA20 blend had volume-based CO emissions of 0.152, 0.171, 0.194, and 0.133%. In the diesel/SSCOME blend, methyl acetate decreased CO emissions more than in the D50/SCOME50 blend. Methyl acetate aids CO-to-$CO_2$ conversion because it transports extra $O_2$ during combustion [38]. It's found that the CO emission at 23° bTDC was 0.161% vol., 0.326% vol., and 0.912% vol., respectively, when considering the EGR percentages of 10%, 15%, and 20%. Similarly, at FITs of 21° bTDC and 19° bTDC, the

CO was 0.217% vol., 0.343% vol., 1.231% vol., 0.244% vol., 0.374% vol., and 1.613% vol., respectively, at EGR rates of 10%, 15%, and 20%. With delayed FIT, CO levels increased but decreased with higher EGR rates. CO climbed 3.5% when the FIT was shortened from 23°bTDC to 19°bTDC at 10% EGR. Due to a shorter delay period, the A/F combination had less duration, potentially boosting CO emissions. However, increasing EGR frequency greatly lowered CO generation [39]. In a specific scenario of FIT 23°bTDC, increasing the EGR from 10% to 20% resulted in a 60% increase in CO. EGR's reduced air input may have generated an oxygen-deficient combustion zone, limiting CO oxidation. Lower gas temperatures reduced the OH-reactive concentration. However, increasing EGR frequency greatly lowered CO generation [40].

### *Smoke opacity*

Figure 3d shows the D50SCOME30MA20 mix SO at different FITs and EGRs. Diesel, D70SCOME30, D50SCOME50 mix, and D50SCOME30MA20 blend had SO at specified power levels of 57.4%, 64.2%, 60.8%, and 51.2%, respectively. The ternary mix has far lower smoke opacity than the binary form. Alcohol has inherent $O_2$ molecules that provide $O_2$ for combustion, reducing smoke [34]. At 23° bTDC SO, EGR levels of 10%, 15%, and 20% were 52%, 62.5%, and 83.2%, respectively. For FITs of 21° and 19° bTDC, the smoke opacity was 56.9%, 66.5%, 88.7%, 61.2%, 69.2%, and 92.5% at EGR rates of 10%, 15%, 20%, respectively. The ternary variant's changes increased smoke production compared to the default. At 10% EGR, decreasing FIT by 23° to 19° bTDC increased SO by 15%. Due to reduced in-cylinder gas pressures during delayed intake latency, the A/F proportion changes. This increases smoke from carbon oxidation [5]. Even more than the FIT delay, rising EGR levels raised SO. Increasing EGR from 10% to 20% at 23° bTDC increased SO by 62.5%. Increased exhaust gas recirculation due to decreasing O2 levels hinders combustion [36].

## MLAs prediction analysis

In this study, the application of deep learning, namely the LSTM model, is utilized as the optimization framework. LSTM was used to predict BTE, BSFC, CO, HC, smoke, and NOx using FIT and EGR variables. First, we train the LSTM model with 288 experimental observations. The network's performance was evaluated using a training dataset of 80% of the experimental data, a validation dataset of 10%, and a testing dataset of 10%. These may be assessed using training and testing of *MRE* and $R^2$-values. After that, the stored network generates output values for the 25 randomly picked input values. Eq. (2) illustrates the correlation coefficient ($R^2$), while Eq. (3) illustrates the *MRE*. Where 'ti' is the target value and 'oi' is the theoretical output value,

$$R^2 = 1 - \left( \frac{\sum_{i=1}^{n} (t_i - \sigma_i)^2}{\sum_{i=1}^{n} (\sigma_i)^2} \right) \quad (2)$$

$$MRE = \frac{1}{n} \sum_{i=1}^{n} \left| 100 \cdot \frac{(t_i - \sigma_i)}{t_i} \right. \quad (3)$$

Let $t_i$ and $o_i$ represent the predicted and measured values, respectively. $t$ denotes the mean of the measured values, while $n$ represents the observations. This method contains knowledge of a particular model's anticipating power regarding a certain dataset. The coefficient of determination, denoted as $R^2$, has a range of values from 0 to 1. An $R^2$ number nearing 1 signifies a higher level of performance [41].

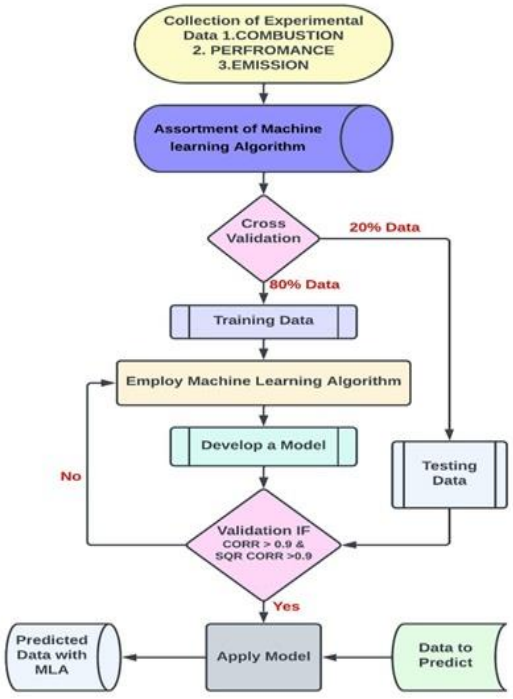


*Figure 4. Machine learning algorithm models flow chart.*

## Evaluation of prediction models

$R^2$ levels are calculated by altering the quantities of training and evaluating information. The $R^2$ for various training and assessment information proportions demonstrates that the model is consistent beyond 80:20 ratios. The score approaching 100% indicates that the model can reflect all variance in output information. The hypothesized approach is contrasted to the $R^2$ values of models developed with

linear regression, support vector machine, neural networks, *K*-nearest neighbors (K-NN), and Deep Learning (LSTM) approaches. Figure 5a depicts model evaluations according to the $R^2$ value. The suggested model surpasses the previous approaches and yields excellent outcomes. The LR, NN, SVM, and LSTM models best fit the narrative or hypothesis of the current examination. At the same time, Figure 5a includes a broad comparison to provide a comprehensive overview of machine learning models. Four distinct ML models predicted values are close to unity. K-NN, PR, GP, and RVM models predicted values are very low compared to the unity. Therefore, this model is not suitable for the current investigation. The $R^2$ values were determined to be 0.92 and 0.96, respectively. The results of the LSTM replication demonstrate its capacity to anticipate crucial features accurately. The *MRE* values for the stated features range from 1.74% to 4.68%, Figure 5b shows that FIT, EGR, BTE, BSFC, and NOx strongly correlate with the target column. Even little changes in these variables affect the target column. CO, HC, and smoke are weaker but favorably connected to the target column. Thus, changes in these columns may not impact the target column. FIT, EGR, BTE, BSFC, and NOx predict the target column well, while CO, HC, and smoke do not. In future modeling and analysis, knowing how qualities relate to the target variable is vital.

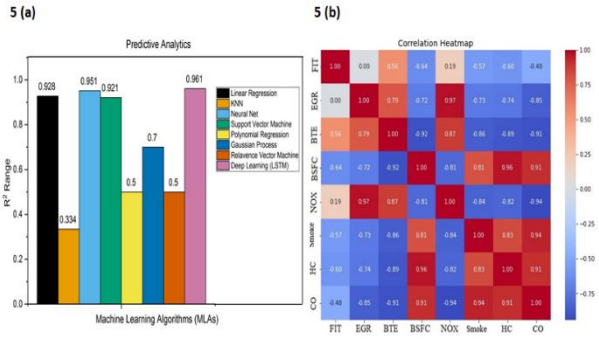


*Figure 5. (a) Comparison of $R^2$ value and 5 (b) Heatmap representing correlation for Machine Learning Algorithms.*

### Validation of the LSTM model

The methodology's practicality must be validated before deployment. The Long Short-Term Memory (LSTM) model improved engine operating settings for experimental studies. The program generated expected significance levels from replications during failure periods. Figure 4 illustrates the training process through a flow chart, and Table 3 was used to verify these results. Eq. (4) calculates the value error percentage.

$$\text{Percentage of error}(\%E) = \frac{\text{Observed value-Predicted value}}{\text{Observed value}} \cdot 100 \quad (4)$$

The best results can only be obtained through appropriate verification. To account for LSTM fuel injection time (FIT) and EGR, the largest input variable maintained from testing was the mean. Equation error rates range from 0.2 to 5.7%. The analysis found fewer than 6% inaccuracies in emissions and efficiency projections. LSTM makes it easier to understand how elements interact. Thus, the Long Short-Term Memory (LSTM) model may predict diesel engine characteristics. Machine learning algorithms may predict pollutants and operational factors. Other quantitative and computational methods may struggle with the problem's complexity and diversity.

## CONCLUSION

The research work outlines the methyl acetate, FIT, and EGR settings affect CI engine parameters in diesel and SCOME variations, as found below.

MA20 injected at 21°bTDC, and 10% EGR had the highest BTE (33%), correlating with the remaining operating conditions. However, the BTE was somewhat lower than that of the MA20 blend at default settings. In MA20 fuel, 21°bTDC and 10% exhaust gas recirculation reduce nitrogen oxides in comparison to other fuels. The MA20 mix decreases the SO by 11% at 21°bTDC and 10% exhaust gas recirculation. However, it was 1% less than baseline diesel. Later, FIT and higher EGR resulted in increased hydrocarbon and CO outflow. The LSTM methods estimate engine output characteristics that are close to unity. LSTM showed the highest R2 and MRE values, which are 0.961 and 1.74%, respectively. All measurements combined show that the other algorithms predict engine responses the least. When considering various injection timings and EGR rates with the MA20 mix, 21° bTDC and 10% EGR are generally the best operating conditions. The results suggest that a Simmondsia Chinensis seed biodiesel mix with MA20 volume can reduce pollutants in CRDI CI engine applications.

Choosing the best fuel injection time and EGR rate to reduce NOx and smoke emissions depends on many parameters, including engine type, fuel properties, and engine performance. According to the provided facts, decreasing emissions may begin with delayed fuel injection from 23º to 19º bTDC. In contrast, brake thermal efficiency, fuel consumption, and engine power output should be considered when selecting optimal operating conditions. Balancing emissions reduction and engine performance is essential. The delayed injection resulted in a decrease in NOx, which in turn led to a reduction in engine performance. Therefore, to evaluate emissions and performance, we

suggest conducting a series of tests or simulations under 21º bTDC at 10% EGR [42,43].

## NOMENCLATURE

| | |
|---|---|
| *ASTM* | American Society for Testing and Materials |
| *bTDC* | Before Top Dead Centre, CA |
| *BSFC* | Brake Specific Fuel Consumption (kg/kW-hr) |
| *BTE* | Brake Thermal Efficiency, % |
| *CA* | Crank Angle, deg |
| *CI* | Cetane Index |
| *CR* | Compression Ratio |
| *CRDI* | Common Rail Direct Injection |
| *CV* | Calorific value |
| *SCOME* | Simmondsia Chinensis Oil Methyl Ester |
| *MA* | Methyl Acetate |
| *D70SCOME30* | Diesel-70%, SCOME-30% |
| *D50SCOME50* | Diesel-50%, SCOME -50% |
| *D50SCOME30MA20* | Diesel-50%, SCOME - 30%, Methyl Acetate - 20% |
| *ECU* | Electronic Control Unit |
| *VCR* | Variable Compression Ratio |
| *HC* | Hydrocarbons, ppm |
| *CO* | Carbon monoxide, % vol. |
| *HRR* | Heat Release Rate, J/deg |
| *ICP* | In-cylinder pressure, bar |
| *NOx* | Nitrogen oxides, ppm |
| *PPM* | Parts Per Million |
| *MLAs* | Machine Learning Algorithms |
| *LSTM* | Long Short-Term Memory |
| *NO* | Neural Network |
| *LR* | Linear Regression |
| *SVM* | Support Vector Machine |
| *KNN* | K-Neural Network |
| *PR* | Polynomial Regression |
| *GP* | Gaussian Process |
| *RVM* | Relative Vector Machine |
| $R^2$ | Squared Correlation |
| *MORE* | Mean Relative Error |
| *RMSE* | Root Mean Square Error |

## REFERENCES


[1] B. Ashok, K. Nanthagopal, B. Saravanan, K. Azad, D. Patel, B. Sudarshan, R.Aaditya Ramasamy, Fuel 235 (2019) 984–994. https://doi.org/10.1016/j.fuel.2018.08.087.

[2] M.M. Khan, R.P. Sharma, A.K. Kadian, S.M.M. Hasnain, Mater. Sci. Energy Technol. 5 (2022) 81–98. https://doi.org/10.1016/j.mset.2021.12.004.

[3] M. Jayapal, K.G. Radhakrishnan, Energy Environ. 33 (2022) 85–106. https://doi.org/10.1177/0958305X20985618.

[4] D. Damodharan, A.P. Sathiyagnanam, B. Rajesh Kumar, K.C. Ganesh, Environ. Sci. Pollut. Res. 25 (2018) 13611–13625. https://doi.org/10.1007/s11356-018-1558-5.

[5] M.V. De Poures, K. Gopal, A.P. Sathiyagnanam, B. Rajesh Kumar, D. Rana, S. Saravanan, D. Damodharan, Energy Sources, Part A. 42 (2020) 1772–1784. https://doi.org/10.1080/15567036.2019.1604888.

[6] M. Arulprakasajothi, N. Beemkumar, J. Parthipan, N. Raju Battu, Arab. J. Sci. Eng. 45 (2020) 563–574. https://doi.org/10.1007/s13369-019-04294-8.

[7] C. Ramakrishnan, P.K. Devan, R. Karthikeyan, Environ. Prog. Sustain. Energy 36 (2017) 248–258. https://doi.org/10.1002/ep.12484.

[8] K. Viswanathan, A. Paulraj, Energy Sources, Part A 45 (2023) 3216–3230. https://doi.org/10.1080/15567036.2020.1849451.

[9] A.I. EL-Seesy, Z. He, H. Hassan, D. Balasubramanian, Fuel 279 (2020) 118433. https://doi.org/10.1016/j.fuel.2020.118433.

[10] J. Preuß, K. Munch, I. Denbratt, Fuel 216 (2018) 890–897. https://doi.org/10.1016/j.fuel.2017.11.122.

[11] S. Raja. K.S, S.K. Srinivasan, K. Yoganandam, M. Ravi, Energy Sources, Part A (2021) 1–11. https://doi.org/10.1080/15567036.2021.1877372.

[12] Y.S.M. Altarazi, A.R. Abu Talib, J. Yu, E. Gires, M.F. Abdul Ghafir, J. Lucas, T. Yusaf, Energy 238 (2022) 121910. https://doi.org/10.1016/j.energy.2021.121910.

[13] R. Jayabal, S. Subramani, D. Dillikannan, Y. Devarajan, L. Thangavelu, M. Nedunchezhiyan, G. Kaliyaperumal, M.V. De Poures, Energy 250 (2022) 123709. https://doi.org/10.1016/j.energy.2022.123709.

[14] M. Miya, K. Venkateswarlu, Int. J. Ambient Energy 43 (2022) 4870–4877. https://doi.org/10.1080/01430750.2021.1923570.

[15] A. Cakmak, M. Kapusuz, O. Ganiyev, H. Ozcan, Environ. Clim. Technol. 22 (2018) 55–68. https://intapi.sciendo.com/pdf/10.2478/rtuect-2018-0004.

[16] V. Praveena, U. Akshaykumar, T. Nishad, J. Phys. Conf. Ser. 2054 (2021) 012050. https://iopscience.iop.org/article/10.1088/1742-6596/2054/1/012050.

[17] M.V. De Poures, A.P. Sathiyagnanam, D. Rana, B. Rajesh Kumar, S. Saravanan, Appl. Therm. Eng. 113 (2017) 1505–1513. https://doi.org/10.1016/j.applthermaleng.2016.11.164.

[18] R. Shanmugam, D. Dillikannan, G. Kaliyaperumal, M.V. De Poures, R.K. Babu, Energy Sources, Part A 43 (2021) 3064–3081. https://doi.org/10.1080/15567036.2020.1833112.

[19] D. Dillikannan, D. J., M.V. De Poures, G. Kaliyaperumal, A.P. Sathiyagnanam, R.K. Babu, N. Mukilarasan, Energy Sources, Part A 42 (2020) 1375–1390. https://doi.org/10.1080/15567036.2019.1604853.

[20] B. Rajesh Kumar, S. Saravanan, Fuel 170 (2016) 49–59. https://doi.org/10.1016/j.fuel.2015.12.029.

[21] J.C. Ge, G. Wu, B.-O. Yoo, N.J. Choi, Energy 253 (2022) 124150. https://doi.org/10.1016/j.energy.2022.124150.

[22] X. Duan, Z. Xu, X. Sun, B. Deng, J. Liu, Energy 231 (2021) 121069. https://doi.org/10.1016/j.energy.2021.121069.

[23] D. Kulandaivel, I.G. Rahamathullah, A.P. Sathiyagnanam, K. Gopal, D. Damodharan, D.P. Melvin Victor, Fuel 278 (2020) 118304. https://doi.org/10.1016/j.fuel.2020.118304.

[24] Y. Yu, Y. Wang, J. Li, M. Fu, A.N. Shah, C. He, IEEE Access 9 (2021) 11002–11013. https://doi.org/10.1109/ACCESS.2021.3050165.

[25] R. Yang, T. Xie, Z. Liu, Energies 15 (2022) 3242. https://doi.org/10.3390/en15093242.

[26] Ü. Ağbulut, M. Ayyıldız, S. Sarıdemir, Energy 197 (2020) 117257. https://doi.org/10.1016/j.energy.2020.117257.

[27] I. Portugal, P. Alencar, D. Cowan, Expert Syst. Appl. 97 (2018) 205–227. https://doi.org/10.1016/j.eswa.2017.12.020.

[28] M. Aliramezani, C.R. Koch, M. Shahbakhti, Prog. Energy

Combust. Sci. 88 (2022) 100967. https://doi.org/10.1016/j.pecs.2021.100967.

[29] W.R. Liao, J.H. Shi, G.X. Li, J. Appl. Fluid Mech. 16 (2023) 2041–2053. https://doi.org/10.47176/jafm.16.10.1801.

[30] M. Vijayaragavan, B. Subramanian, S. Sudhakar, L. Natrayan, Int. J. Hydrogen Energy 47 (2022) 37635–37647. https://doi.org/10.1016/j.ijhydene.2021.11.201.

[31] B. Ashok, K. Nanthagopal, M. Senthil Kumar, A. Ramasamy, D. Patel, S. Balasubramanian, S. Balakrishnan, Int. J. Green Energy 16 (2019) 834–846. https://doi.org/10.1080/15435075.2019.1641107.

[32] H. Xiao, X. Yang, R. Wang, S. Li, J. Ruan, H. J, Therm. Sci. 24 (2020) 215–229. https://doi.org/10.2298/TSCI190112304X.

[33] M. Chandran, R. Chinnappan, C. Kit Ang, Energy Sources, Part A (2020) 1–13. https://doi.org/10.1080/15567036.2020.1764671.

[34] G.R. Kothiwale, K.M. Akkoli, B.M. Doddamani, S.S. Kattimani, Ü. Ağbulut, A. Afzal, A.R. Kaladgi, Z. Said, Int. J. Environ. Sci. Technol. 20 (2023) 5013–5034. https://doi.org/10.1007/s13762-022-04397-0.

[35] K. Subramanian, S.A. Paramasivam, D. Dillikannan, M. Muthu, P.R. Yadav Sanjeevi, Int. J. Ambient Energy (2022) 1–14. https://doi.org/10.1080/01430750.2022.2103184.

[36] B. Rajesh Kumar, S. Saravanan, D. Rana, A. Nagendran, Energy Convers. Manage. 123 (2016) 470–486. https://doi.org/10.1016/j.enconman.2016.06.064.

[37] B. Ashok, K. Nanthagopal, R.T.K. Raj, J. P. Bhasker, D. Sakthi Vignesh, Fuel Process. Technol. 167 (2017) 18–30. https://doi.org/10.1016/j.fuproc.2017.06.024.

[38] B.R. Kumar, S. Saravanan, Fuel 180 (2016) 396–406. https://doi.org/10.1016/j.fuel.2016.04.060.

[39] K. Duraisamy, R. Ismailgani, S.A. Paramasivam, G. Kaliyaperumal, D. Dillikannan, Energy Environ. 32 (2021) 481–505. https://doi.org/10.1177/0958305X20942873.

[40] A. Ramesh, B. Ashok, K. Nanthagopal, M. Ramesh Pathy, A. Tambare, P. Mali, P. Phuke, S. Patil, R. Subbarao, Fuel 249 (2019) 472–485. https://doi.org/10.1016/j.fuel.2019.03.072.

[41] A.E. Gürel, Ü. Ağbulut, Y. Biçen, J. Cleaner Prod. 277 (2020) 122353. https://doi.org/10.1016/j.jclepro.2020.122353.

[42] M.V. De Poures, D. Dillikannan, G. Kaliyaperumal, S. Thanikodi, Ü. Ağbulut, A.T. Hoang, Z. Mahmoud, S. Shaik, C .A.Saleel, A.Afzal Process Saf. Environ. Prot. (2023), 738–752, https://doi.org/10.1016/j.psep.2023.02.054.

[43] D. Kulandaivel, I.G. Rahamathullah, A.P, Sathiyagnanam, K. Gopal , D. Damodharan, De Poures Melvin Victor, Fuel, 278, (2020), https://doi.org/10.1016/j.fuel.2020.118304.

KARTHIKEYAN SUBRAMANIAN[1]

SATHIYAGNANAM AMUDHAVALLI PARAMASIVAM[2]

DAMODHARAN DILLIKANNAN[3]

[1]Department of Mechanical Engineering, Annamalai University, Chidambaram, Tamil Nadu, India

[2]Department of Mechanical Engineering, Govt. College of Engineering (Deputed from Annamalai University), Salem, Tamil Nadu, India

[3]Department of Mechanical Engineering, Jeppiaar Engineering College, Chennai, Tamil Nadu, India

NAUČNI RAD

# PREDVIĐANJA MAŠINSKOG UČENJA O IZLAZNIM PARAMETRIMA MOTORA SA COMMON RAIL DIREKTNIM UBRIZGAVANJEM GORIVA TERNARNE MEŠAVINE

*Cilj ovog rada je da algoritmom mašinskog učenja (MLA) predvidi emisije CRDI (common rail direktno injektor) motora i performansi koristeći alternativnu sirovinu. Istraživanja su započeta trokomponentnom mešavinom dizel-SCOME-metil acetat. Motor je testiran sa vremenom ubrizgavanja goriva (FIT) od 23°, 21° i 19° bTDC sa nivoima recirkulacije izduvnih gasova (EGR) od 10%, 15% i 20% pri procenjenoj produktivnosti snage. Usporavanje vremena ubrizgavanja i povećanje EGR-a smanjuju vršni pritisak u cilindru. Radni uslovi sa maksimalnim BTE su bili 21° bTDC i 10% EGR. Podešavanje vremena ubrizgavanja i EGR smanjilo je azot oksid u odnosu na osnovnu liniju. Prozirnost dima bila je 1% niža na 21° bTDC i 10% recirkulacije izduvnih gasova nego u konvencionalnom dizel pogonu. Usporeno vreme ubrizgavanja i recirkulacija izduvnih gasova povećavaju emisije HC i CO. Međutim, MLA predviđa rad motora CI i svojstva pražnjenja. Model dugotrajne kratkoročne memorije (LSTM) predviđa izlazne karakteristike motora sa korelacijom na kvadrat ($R^2$) od 0,92 do 0,96. Istovremeno, vrednosti srednje relativne greške (MRE) kretale su se od 1,7 do 4,7%. Ovi rezultati pokazuju da LSTM modeli pružaju superiorne prediktivne mogućnosti, posebno kada se razmatraju brojne promenljive za analizu reakcija motora.*

*Ključne reči: gusta membrana; prozračna membrana; stepen apsorpcije; propustljivost biodizel; metil acetat; CRDI motor; EGR; algoritmi mašinskog učenja.*